

Shell formation and nuclear masses

A.P. Zuker

IPHC, IN2P3-CNRS, Université Louis Pasteur,
F-67037 Strasbourg, France,
e-mail:Andres.Zuker@IReS.in2p3.fr

Recibido el 4 de marzo de 2008; aceptado el 14 de abril de 2008

We describe the basic mechanisms responsible for nuclear bulk properties and shell formation incorporated in the Duflo Zuker models. The emphasis is put on explaining why functionals of the occupancies can be so efficient in accounting for data with minimal computational effort.

Keywords: Binding energies and masses.

Se discuten los mecanismos que son responsables para la propiedades nucleares globales y la formación de capas en los modelos Duflo-Zuker. Se enfatiza la importancia de funcionales de las ocupancias para describir los datos experimentales con un esfuerzo computacional mínimo.

Descriptores: Energías de amarre y masas.

PACS: 21.10.Dr

It is commonly asserted that whenever shell model (SM) calculations become untractable—*i.e.*, mostly everywhere in the periodic table—they should be replaced by mean field (MF), or better, density functional theory (DFT) treatments. The implicit (and unstated) assumption is that MF or DFT must in some sense be equivalent to SM—*i.e.*, to solving the Schrödinger equation—but much simpler. The Duflo Zuker mass model [1] occupies a special position:

- It is not a MF.
- It is not a DFT but a functional of orbital occupancies.
- It follows explicitly the steps involved in solving the Schrödinger equation.
- It is computationally trivial when compared with other mass models, and gives much better agreement with measured values.
- It is almost universally claimed that the model is incomprehensible, which has retarded its acceptance.

Let me try to make it comprehensible by steps. First we look at Fig. 1 which shows experimental binding energies [4] subtracted from the Bethe Weizsäcker liquid drop (LD) form in Eq. (1) with a subtle modification: A reasonable fit to the data with root-mean-square deviation of some 2.5 MeV is achieved with a “pairing energy” $V_p=5.15[\text{mod}(N, 2)+\text{mod}(Z, 2)]A^{-1/3}$; which means that the information coming from any of the four mass sheets (even-even, even-odd, odd-even and odd) is basically the same; hence from now on, we examine only even-even nuclei. Then V_p becomes irrelevant: The subtle modification is to replace it by a shift of $-A^{1/3}$ MeV. It is seen that the result is to displace the whole energy patterns so as to make

the shell effects practically definite positive, thus defining a convenient “baseline”.

$$E(LD) = 15.5A - 17.8A^{2/3} - 28.6 \frac{4T(T+1)}{A} + 40.2 \frac{4T(T+1)}{A^{4/3}} - \frac{.7Z(Z-1)}{A^{1/3}} - V_p, \quad (1)$$

It only remains to read Fig. 1 to have a good mass formula as a sum of a macroscopic baseline plus shell effects represented by quadratic, cubic and quartic terms in the number of active protons and neutrons in spaces defined by magic numbers, basically 28, 50, 82 and 126. This was achieved with great success by Jean Duflo [2] under a slightly different guise from the one described here. In a companion paper [3] it was shown that it should be possible to derive microscopically something quite close to Duflo’s formula.

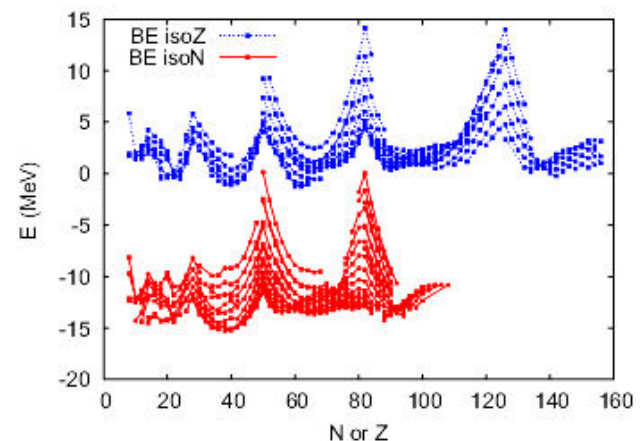


FIGURE 1. (Color online) Shell effects ($BE(\text{exp})-E(\text{LD})$) along isotope and isotone lines (latter displaced by -14 MeV). Only even-even shown. PLEASE READ TEXT CAREFULLY.

There were serious problems though: no clearcut definition of the baseline, need to postulate the magic numbers as well as the transition points between spherical and deformed regions. (The latter show as flat patterns at the bottom of the parabolas in Fig. 1. All these problems were solved in Ref. 1, and it is convenient to make a list of what are the injunctions defining this work

- Separate LD from shell effects.
- Separate deformed from spherical.
- Separate Hartree Fock (HF) from correlations.
- Be very careful about scaling; *i.e.* recognize what goes as $A, A^{2/3}, A^{1/3}, A^0, A^{-1/3}$. In particular
- Be uncompromising about LD principles:
 1. Pairing scales as $A^{-1/3}$, NOT $A^{-1/2}$ [5]
 2. Coulomb is in $Z(Z - 1)$. NOT Z^2 [6]
 3. Symmetry is in $T(T + 1)$, NOT $(N - Z)^2$ [7]
 4. Shell effects scale as $A^{1/3}$.

Now we proceed as we would in solving the Schrödinger equation, and define a good unperturbed, monopole, Hamiltonian. We refer to Ref. 7 for details and arguments on the matter. Here, it is sufficient to know that we start with a set of matrix elements in an isospin coupling scheme

$$W_{rstu}^{JT} = V_{rstu}^{JT} - \delta_{rt}\delta_{su}V_{rs}^T. \quad (2)$$

from which we have extracted centroids

$$V_{rs}^T = \frac{\sum_J V_{rsrs}^{JT}[J](1 - (-1)^{J+T}\delta_{rs})}{(2j_r + 1)(2j_s + 1 + \delta_{rs}(-1)^T)} \quad (3)$$

In the neutron-proton (np) scheme each orbit r goes into two r_n and r_p and the centroids can be obtained through $(x, y = n \text{ or } p, x \neq y)$

$$V_{r_x s_y} = \frac{1}{2} \left[\mathcal{V}_{rs}^1 \left(1 - \frac{\delta_{rs}}{2j_r + 1} \right) + V_{rs}^0 \left(1 + \frac{\delta_{rs}}{2j_r + 1} \right) \right] \quad (4)$$

$$V_{r_x s_x} = V_{rs}^1.$$

The monopole Hamiltonian is then a quadratic form in number operators m_{rx}

$$H_m^d = K^d + \frac{1}{2} \sum_{r_x, s_y} V_{r_x s_y} m_{r_x} (m_{s_y} - \delta_{r_x s_y} \delta_{xy}) \quad (5)$$

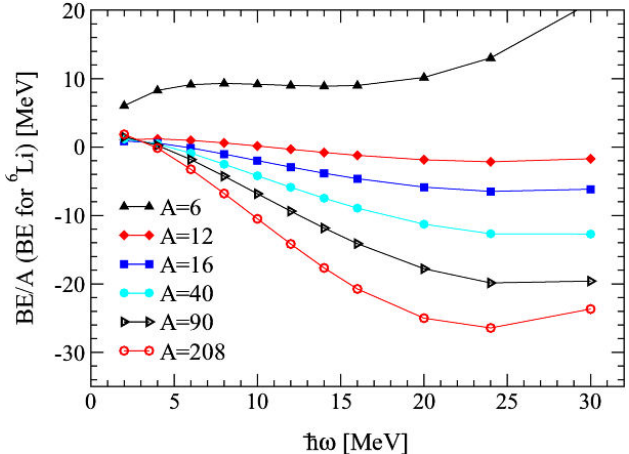


FIGURE 2. Ground state energies per particle (except for ${}^6\text{Li}$) obtained from Eq. (5) (Coulomb included schematically) by filling lowest oscillator orbits.

where we have added the kinetic energy. Fig. 2 shows some binding energies obtained from Eq. (5) using a $V_{\text{low } k}$ potential [8]. At low density (*i.e.*, low $\hbar\omega$) the interaction behaves as a contact δ force and the energies go as $(\hbar\omega)^{3/2}$. At high density the interaction behaves as a constant, the kinetic energy dominates, and the system saturates, but at totally wrong places: the right saturation minima should come around the standard value $\hbar\omega \approx 40A^{-1/3} \approx 6 - 15$ MeV. In this range the energy is linear in $\hbar\omega$. When nocore SM calculations are performed [9] the gain in energy is substantial but the patterns in the figure are preserved. Therefore better calculations do not lead to saturation which has to be enforced artificially through use of the correct $\hbar\omega$, as done in SM work. In the future it would be better to do it through three-body forces as explained in Ref. 7 (around pag. 436).

The master terms

Now we invoke the general factorization property [5]

$$\sum_{x,y} V_{xy} Z_x \cdot Z_y = \sum_{\mu} E_{\mu} \left(\sum_k Z_k f_{k\mu} \right)^2 \quad (6)$$

and apply it to Eq. (5), or its equivalent in isospin formalism, so Z are operators $Z \equiv m, T$. By diagonalizing realistic monopole centroids over many oscillator shells one finds that the strong isoscalar and isovector collective—master—terms that overwhelm all others are of the form

$$\mathcal{V}^{d0} = E^0 \left(\sum_p \frac{m_p}{\sqrt{D_p}} \right)^2, \quad \mathcal{V}^{d1} = E^1 \left(\sum_p \frac{T_p}{\sqrt{D_p}} \right)^2 \quad (7)$$

where $D_p = (p + 1)(p + 2)$ is the degeneracy of the major harmonic oscillator (HO) shell of principal quantum number p . Setting $E^T = \hbar\omega\mathcal{V}^T$, using Boole's notation $p^{(3)} = p(p - 1)(p - 2)$, and summing up to the Fermi shell p_f

we obtain asymptotic estimates

$$\sum_p m_p = \sum_{p=0}^{p_f} 2D_p = A = \frac{2(p_f + 3)^{(3)}}{3}. \quad (8)$$

$$\begin{aligned} \mathcal{K}^d &= \frac{\hbar\omega}{2} \sum_p m_p(p + 3/2) \\ &\Rightarrow \frac{\hbar\omega}{4} (p_f + 3)^{(3)} (p_f + 2) \end{aligned} \quad (9)$$

$$\langle r^2 \rangle = \frac{\hbar}{AM\omega} \sum_p m_p(p + 3/2) \Rightarrow \frac{3\hbar}{4M\omega} (p_f + 2) \quad (10)$$

$$\mathcal{V}^{d0} \hbar\omega \mathcal{V}_0 \left(\sum_p \frac{m_p}{\sqrt{D_p}} \right)^2 \Rightarrow \hbar\omega \mathcal{V}_0 [p_f(p_f + 4)]^2 \quad (11)$$

Showing that \mathcal{V}^{d0} and \mathcal{K}^d go as A , as they should. A more careful recent fit to the master terms reveals that in Eq. (7) the denominators are better approximated by

$$1/\sqrt{D_p} \rightarrow 1/\sqrt{D_p} - \alpha/D_p,$$

leading asymptotically to surface terms. It is impossible to overestimate what is achieved by the master terms: they simply account for the four LD main terms in Eq. (1), and they produce strong magicity effects at the HO closures.

The S operators and the monopole contribution

The problem we must face next is to erase most of the HO closures and turn them into extruder-intruder (EI) ones as explained schematically in Fig. 3. The D_p levels in HO shell p are split in two groups: the largest subshell $j(p) \equiv p_>$ with

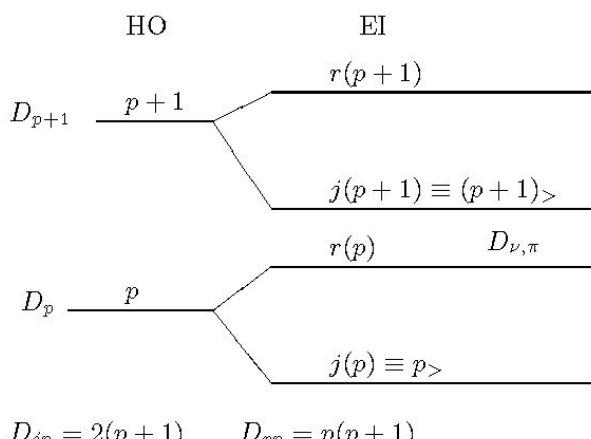


FIGURE 3. HO and EI closures

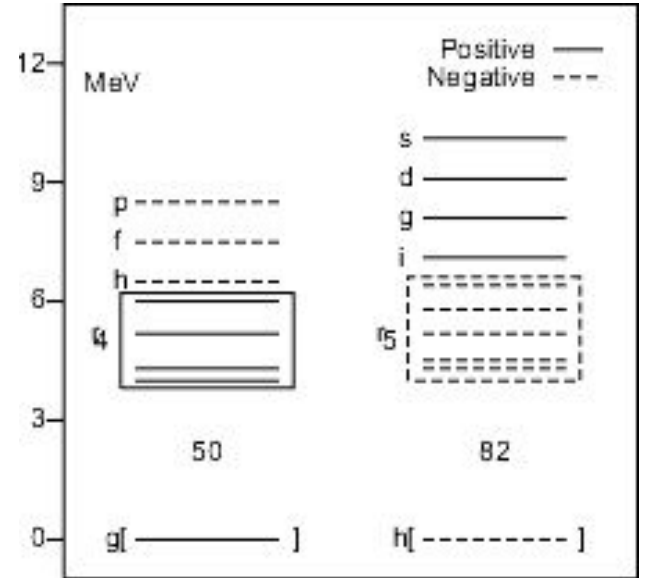


FIGURE 4. Schematic single particle spectrum above ^{132}Sn . r_p is the set of orbits in shell p excluding the largest. For the upper shells the label l is used for $j = l + 1/2$

$j=p+1/2$, $D_p=2(p+1)$, and the rest $r(p)$ with $D_{rp}=p(p+1)$. The largest shell $j(p)$ is extruded from major shell p and intrudes in major shell $p-1$. Clearly $m_p=m_{rp}+m_{p_>}$, and we must supplement the master term with others containing operators other than m_p . The natural choice is

$$S_p = (pm_{p_>} - 2m_{r_p}) = \frac{D_{rp}m_{p_>} - D_{p_>}m_{r_p}}{(p+1)}, \quad (12)$$

which vanishes at HO closures. Similar terms can be constructed for the isospin operators ST_p .

By now we are ready to propose a schematic monopole contribution made of all possible symmetric quadratics in m_p , S_p , T_p , ST_p .

Spherical correlations

To this we must add the effect of spherical correlations. In Ref. 3 it is shown how to invoke perturbation theory or coupled cluster theory and average to obtain the corresponding estimates, as in the following example, involving a quadrupole-quadrupole np interaction in the EI spaces (any other multipole would do; number operators defined at bottom of Fig. 3)

$$\begin{aligned} \langle H_m^{eff} \rangle &= \chi C \langle nz | q_\pi \cdot q_\nu q_\pi \cdot q_\nu | nz \rangle \\ &= \chi C \langle z | q_\pi \cdot q_\pi | z \rangle \langle n | q_\nu \cdot q_\nu | n \rangle \end{aligned} \quad (13)$$

Upon averaging this four-body operator must go as $n_\pi(D_\pi - n_\pi)n_\nu(D_\nu - n_\nu)$, as dictated by vanishing at empty and closed shells. Note the extreme generality of this argument, that only relies on the possibility of performing averages.

TABLE I. $B(E2) \uparrow$ in $e^2 b^2$ compared with experiment.

N	Nd	Sm	Gd	Dy
92	4.47	4.51	4.55	4.58
	2.6(7)	4.36(5)	4.64(5)	4.66(5)
94	4.68	4.72	4.76	4.80
			5.02(5)	5.06(4)
96	4.90	4.95	4.99	5.03
			5.25(6)	5.28(15)
98	5.13	5.18	5.22	5.26
				5.60(5)

Deformation

In DZ for each nucleus two calculations are performed and the lowest kept. We have just described the ingredients of the spherical case. Deformation is associated with the promotion of four neutrons and four protons to the next major shell. The loss of monopole energy is upset by the gain in quadrupole coherence of the form in Eq. (13). This mechanism, vindicated by the very good description of masses in deformed

regions has been later confirmed by the accurate estimate of quadrupole moments. The story is told in Ref. 7 (around page 464) from which we borrow Fig. 4 showing the orbits being filled above ^{132}Sn . Starting at around Nd ($Z=60$), as the first neutron shell above $N=82$ ($f_{7/2}$) fills, spherical solutions dominate up to $N=90$ where rotational motion sets in. Using SU3-like arguments the intrinsic quadrupole moments and $B(E2)$ rates can be estimated as

$$Q_0 = 56e_\pi + (76+4n)e_\nu, \quad B(E2) \uparrow = 10^{-5} A^{2/3} Q_0^2 \quad (14)$$

for $N=90+2n$ and effective charges $e_\pi=1.4$, $e_\nu=0.6$. Results are given in Table I. (The ^{152}Nd value has now been remeasured...).

The DZ strategy. Three body and surface terms

By now we have obeyed all the injunctions mentioned earlier and we can define the strategy to construct a general monopole functional. It amounts to enumerate all conceptually acceptable terms and then select through numerical fits the indispensable ones,

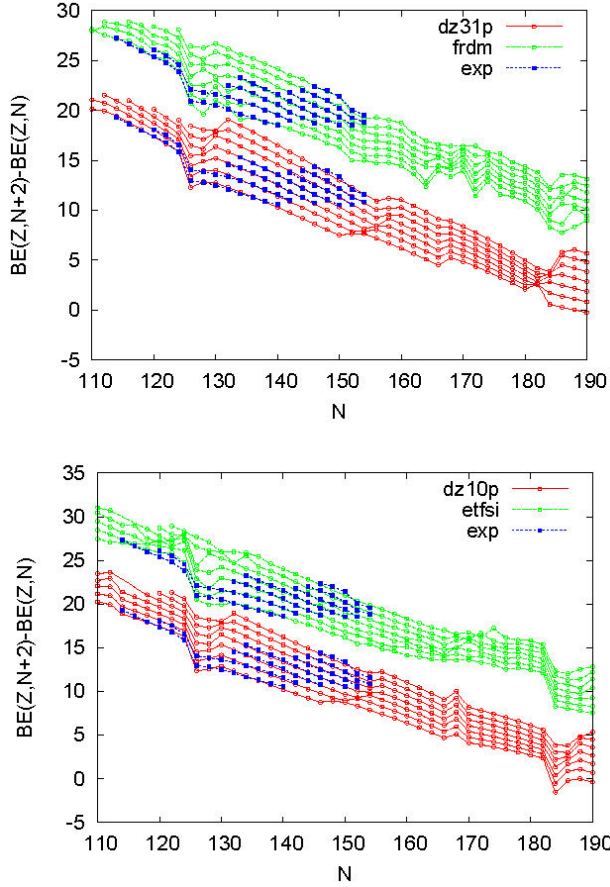


FIGURE 5. Two neutron separation energies for $Z=88-100$ for frdm(rmsd=621 keV) and dz(31p, rmsd=338 keV), and etfsi(rmsd=703 keV) and dz(10p, rmsd=524 keV). frdm displaced up by 8 MeV.

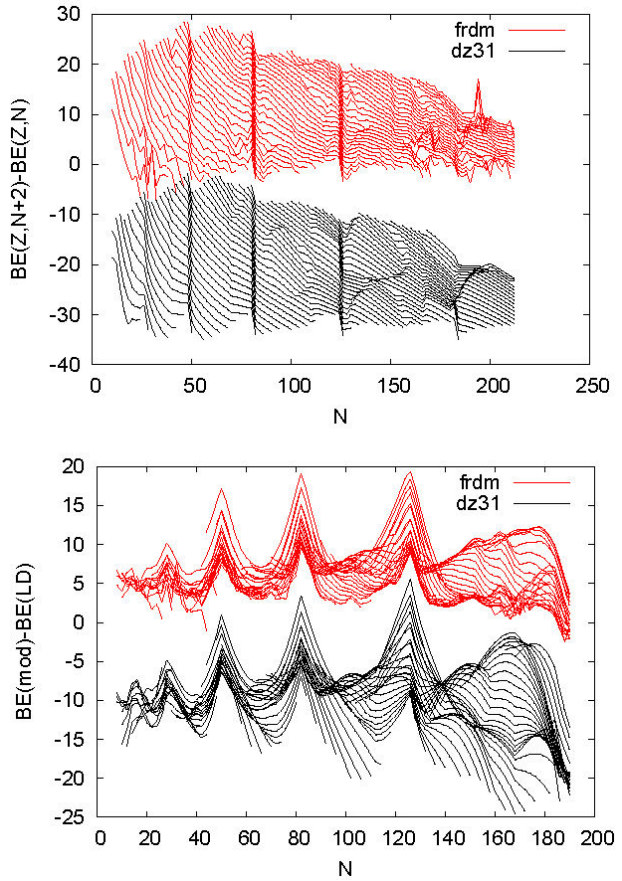


FIGURE 6. Two neutron separation energies and binding energies related to LD in Eq. (1) for frdm and dz(31p), displaced down by 30 and 15 MeV respectively.

- 1 Strict monopole terms: quadratics in number operators.
- 2 Correlation terms: quadratics, cubics and quartics. Note that quadratics have the same form for monopole and correlation.
- 3 Surface terms associated to each of the above, *i.e.*, each operator Γ becomes $\Gamma(1-aA^{-1/3})$, with $a \approx 5$ for most operators, which means they change sign at $A \approx 100$.
- 4 The fits demand an anomalous cubic term $n_\pi(D_\pi-n_\pi)(D_\pi-2n_\pi)+n_\nu(D_\nu-n_\nu)(D_\nu-2n_\nu)$ that scales as A , *i.e.*, it violates the injunction that shell effects should scale as $A^{1/3}$

The number of possible contributions consistent with this enumeration is very large and we have settled for two standard versions:

dz31p A 31 parameter variant of the published 28 parameter fit [1] both to the 1993 data [10]. For the 2003 data [11] dz31p yields rmsd=338 keV (2035 nuclei). Fortran code available on request (some 400 lines).

dz10p The 10 parameter version, rmsd=524 keV to the 2003 data. Fortran code available at Ref. 4.

Figures 5 compares dz31p and dz10p with the finite range droplet model (frdm [12], about 30 parameters, rmsd=521 keV) and extended Thomas Fermi mean field calculations (etfsi, about 10 parameters [13], and references therein; rmsd=703 keV). The $Z=88-100$, $N=110-190$ range has the advantage of including some measured values and reaching the putative $N=184$ EI closure.

Three remarks

- The indications of $N=184$ magicity are almost absent for dz31p, very marginal for frdm and fairly clear for dz10p and etfsi.
- The dz patterns are smooth: beyond $N=126$ magicity, one detects only some anecdotic effects in the $N=160-170$ range.
- The frdm and etfsi patterns are agitated: many things happen in places where nothing happens in dz.

Figure 6 collects predictions for some 8000 nuclei.

Globally the two neutron separation energies for frdm and dz31p are quite similar but again systematically more abrupt in frdm. Worth noting: drip lines are very much the same for both models.

The LD subtracted binding energies are probably the most revealing: The qualitative similarity is striking, especially for the heavier regions about which nothing is known.

The strong dz unbinding for states beyond the drip-lines is suspicious. Difficult to decide whether the hint is interesting or misleading.

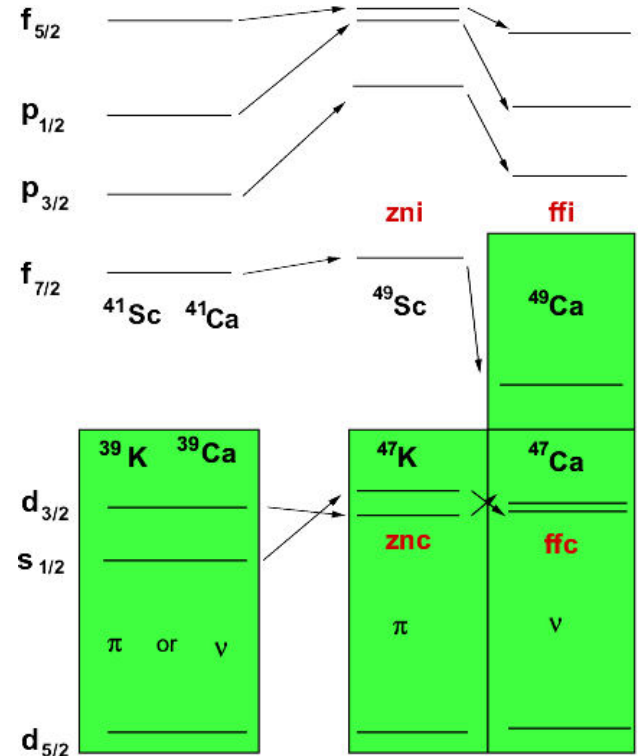


FIGURE 7. Evolution of $(cs \pm 1)$ spectra from ^{40}Ca to ^{48}Ca

As mentioned, the dz “philosophy” was declared at first to be incomprehensible. It is only when the 2003 mass data were published that the predictive power of the approach began to be recognized [15] and dz was accepted as one of the three standards alongside frdm and etfsi (later hfb [13]). There is no point in deciding which is better but it is clear that frdm and etfsi produce too many shell effects that are not there, while dz may be too smooth and miss shell effects that are there. However, I would like to postulate the following

The only fundamental shell effects are related to the appearance and disappearance of EI closures. All other magicity effects are miscellaneous [3]

Blunt as this statement may sound it only amounts to a reading of Fig. 1.

The monopole Hamiltonian and the EI problem [14]

Realistic interactions provide a crucial hint: the master terms. They give no hint about the HO to EI transition: they do not produce EI magicity [8]. Hence, it has to be “invented”; dz31p (dz10p) produce the transition in a complicated (simpler) way. No way to know which is the right one (if any). If now we remember that one of the dz injunctions is to separate monopole (HF) from correlation (SM) we note that dz cannot possibly do it, because the biggest effects are quadratic and—as noted—there is no way to know their origin when

fitting masses. So here we try a more fundamental approach: define autonomously the monopole Hamiltonian. This was attempted quite successfully in Ref. 14, which we shall refer to as dz2. The idea is to separate cleanly LD from shell effects, and then characterize the latter by the particle and hole spectra on closed shells, a set we call $cs \pm 1$. The separation is achieved by the—master minus four times kinetic—combination in Eq. (15) which produces the basic HO magicity, but vanishes to order A and $A^{2/3}$. The mechanism to produce $cs \pm 1$ spectra is illustrated in Fig. 7,

- 1 On HO closures (^{40}Ca in this case) an $l \cdot s + l \cdot l$ one body term produces the right spectrum. The assumption is borne out by realistic forces [8]
- 2 The evolution to EI closures is driven by the $f_{7/2}$ orbit through four types of two body “drift” terms in Eq. (16): intra-shell neutron proton (zni), cross-shell neutron proton (znc), intra-shell nn or pp (ffi), cross-shell nn or pp (ffc). For example, in going from ^{41}Ca to ^{49}Ca the original (basically $l \cdot s$) spectrum must be modified so as to leave unchanged the upper levels (r_3) and depress the $3_>$ *i.e.*, $f_{7/2}$ orbit. In other words the ffi term must contain an operator of the form $m_{3>}S_3$ [see Eq. (12)].

$$W - 4K = \left(\sum_p \frac{m_p}{\sqrt{D_p}} \right)^2 - 2 \sum_p m_p (p + 3/2) \quad (15)$$

$$H_m^s = W - 4K + l \cdot s + l \cdot l + 2b \text{ drift terms} \quad (16)$$

A six parameter fit to some 90 $cs \pm 1$ levels yields $\text{rmsd}=200$ keV. The neutron and proton gaps ($2BE(N, Z) - BE(N+1, Z) - BE(N-1, Z)$, $2BE(N, Z) - BE(N, Z+1) - BE(N, Z-1)$), though not included in the fit, are also accurately reproduced [14]. Fig. 8 illustrates how the evolution takes place in $N=Z$ nuclei:

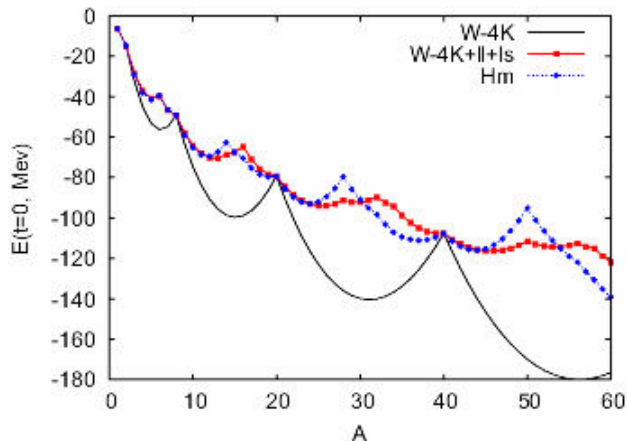


FIGURE 8. The different contributions of Eq. (15) for $N=Z$

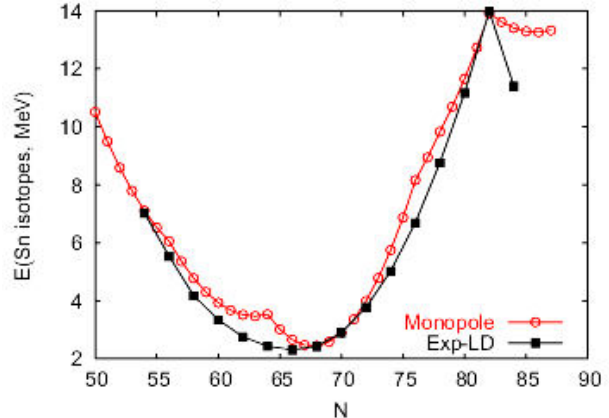


FIGURE 9. LD referred energies of Sn isotopes compared to monopole predictions. Both even and odd N shown for the latter.

- a) $W - 4K$ produces huge HO effects;
- b) $l \cdot s + l \cdot l$ very much erase the HO magicity;
- c) It is the drift terms that eventually drive the EI closures.

Equation 16, collects all the terms. It is worth noting that the drift terms that play such a crucial role in generating EI magicity are small: EI closures may be spectacular but they are fragile.

Though by construction the monopole Hamiltonian in Eq. (16) is free of terms that go as A and $A^{2/3}$, to compare with data we have to correct for $A^{1/3}$ effects (apparent in Fig. 8 for example). Similarly we expect the need of corrections to the symmetry *i.e.*, $T(T+1)$ terms. When this is done we find what is shown in Fig. 9 for the Sn isotopes (the odd N points could be ignored).

The agreement is quite satisfactory, BUT we have omitted the most interesting: once the $A^{1/3}$ and $T(T+1)$ corrections are made the agreement is obtained by reducing the shell effects by a VERY substantial 2.5 factor. This is truly significant, as it stresses the need to separate strict mean field (MF, H_m in Eq. (16)) from correlation effects subsumed in the 2.5 factor. Even if MF may mock such effects globally, it cannot help letting some shell effects to smuggle through, as is the case of the $N=64$ closure in Fig. 9, and as made evident in Figs. 5 and 6. The prevalent idea that the pairing force is what is needed to go beyond MF. This is not so: a SM calculation cannot be mocked simply as MF plus pairing.

Figure 9 is also useful in explaining why dz works. The explanation comes in two steps:

- a) By construction, dz cannot produce subshell effects as the $N=64$ closure.
- b) Even when correlations have erased such effects, there remains a trace of subshell structure as made evident by the experimental pattern for the Sn isotopes that is not a symmetric parabola around the minimum.

This is where the strange cubic and surface terms come in: They mock such effects quite well. We do not know why but it is worth understanding it.

1. Microscopic mass formulas. J. Duflo and A.P. Zuker , *Phys. Rev. C* **52** (1995) R23
2. J. Duflo, *Nucl. Phys. A* **576** (1994) 29.
3. On the microscopic derivation of a mass formula. A.P. Zuker, *Nucl. Phys. A* **576** (1994) 65.
4. www.nndc.bnl.gov; George Audi database, AMDC.
5. The realistic collective Hamiltonian. M. Dufour and A.P. Zuker, *Phys. Rev. C* **54** (1996) 1641.
6. Mirror displacement energies and neutron skins. J. Duflo and A.P. Zuker, *Phys. Rev. C* **66** 051304R (2002).
7. The Shell Model as a Unified View of Nuclear Structure: E. Caurier, G. Martínez-Pinedo, F. Nowacki, A. Poves, A.P. Zuker, nucl-th/0402046. *RMP* **77** (2005) 427-488.
8. Shell-model phenomenology of low-momentum interactions Achim Schwenk and A.P. Zuker, *Phys. Rev. C* **74** (2006) 061302(R).
9. Unpublished nocore SM calculations up to mass 40. E. Caurier, A. Schwenk and A.P. Zuker (2007).
10. G. Audi and A.H. Wapstra *Nucl. Phys. A* **565**, (1993) 1.
11. G. Audi, A.H. Wapstra and C. Thibault *Nuclear Physics A* **729** (2003) 337.
12. P. Möller, J.R. Nix, W.D. Myers and W.J. Swiatecki, *ADNDT* **59** (1995) 185.
13. S. Goriely, M. Samyn, and J.M. Pearson *Phys. Rev. C* **75** (2007) 064312. See also www-astro.ulb.ac.be
14. The Nuclear Monopole Hamiltonian, J. Duflo and A.P. Zuker, *Phys. Rev. C* **59** (1999) 2347R.
15. Recent trends in the determination of nuclear masses D. Lunney, J.M. Pearson and C. Thibault *RMP* **75** (2003) 1021-1082.